

## Article

# Modelling Electricity Consumption in Cambodia Based on Remote Sensing Night-Light Images

Xumiao Gao <sup>1,2</sup> , Mingquan Wu <sup>1,2,\*</sup> , Ju Gao <sup>3</sup>, Li Han <sup>4</sup>, Zheng Niu <sup>1,2</sup>  and Fang Chen <sup>2,5,6</sup>

<sup>1</sup> State Key Laboratory of Remote Sensing Science, Aerospace Information Research Institute, Chinese Academy of Sciences, Beijing 10094, China; gaoxumiao20@mails.ucas.ac.cn (X.G.); niuzheng@radi.ac.cn (Z.N.)

<sup>2</sup> University of Chinese Academy of Sciences, Beijing 10049, China; chenfang@radi.ac.cn

<sup>3</sup> School of Economics and Management, Southwest Forestry University, Kunming 650224, China; gaoj666@yeah.net

<sup>4</sup> School of Civil Engineering, Southwest Forestry University, Kunming 650224, China; hanli2085@swfu.edu.cn

<sup>5</sup> Key Laboratory of Digital Earth Science, Aerospace Information Research Institute, Chinese Academy of Sciences, Beijing 10094, China

<sup>6</sup> International Research Centre of Big Data for Sustainable Development Goals, Beijing 10094, China

\* Correspondence: wumq@aircas.ac.cn

**Abstract:** The accurate estimation of electricity consumption and its spatial distribution are important in electricity infrastructural planning and the achievement of the United Nations Sustainable Development Goal 7 (SDG7). Electricity consumption can be estimated based on its correlation with nighttime lights observed using remote sensing imagery. Since night-light images are easily affected by cloud cover, few previous studies have estimated electricity consumption in cloudy areas. Taking Cambodia as an example, the present study proposes a method for denoising night-light images in cloudy areas and estimating electricity consumption. The results show that an exponential model is superior to linear and power function models for modelling the relationship between total night-light data and electricity consumption in Cambodia. The month-specific substitution method is best for annual night-light image synthesis in cloudy areas. Cambodia's greatest electricity consumption occurs in its four most economically developed cities. Electricity consumption spreads outwards from these cities along the main transport routes to a large number of unelectrified areas.

**Keywords:** night-light image processing in cloudy areas; VIIRS/DNB; estimated electricity consumption; spatial patterns of electricity consumption; SDG7



**Citation:** Gao, X.; Wu, M.; Gao, J.; Han, L.; Niu, Z.; Chen, F. Modelling Electricity Consumption in Cambodia Based on Remote Sensing Night-Light Images. *Appl. Sci.* **2022**, *12*, 3971. <https://doi.org/10.3390/app12083971>

Academic Editor: Filipe Soares

Received: 15 March 2022

Accepted: 12 April 2022

Published: 14 April 2022

**Publisher's Note:** MDPI stays neutral with regard to jurisdictional claims in published maps and institutional affiliations.



**Copyright:** © 2022 by the authors. Licensee MDPI, Basel, Switzerland. This article is an open access article distributed under the terms and conditions of the Creative Commons Attribution (CC BY) license (<https://creativecommons.org/licenses/by/4.0/>).

## 1. Introduction

Electricity is the most dynamic and efficient form of energy [1]. It is one of the main drivers of scientific, technological, and economic development, and is key to the quality of life and economic development in poor countries [2]. The United Nations Sustainable Development Goal 7 (SDG7) roadmap aims to provide affordable, reliable, sustainable, and modern energy services for all by 2030. To achieve this, accurate and timely estimates of electricity consumption and its spatial patterns are important for energy-efficient electricity planning in the region and for achieving SDG7.

When Earth is observed from above at night, the dazzling glow of electric lights in human settlements and economic zones can be easily ascertained. When the sky is cloudless, remote sensing satellites can capture various visible sources of radiation, such as town lights, fishing boat lights, and fires. Images of the Earth's visible lights acquired at night are known as night-light images. From a historical point of view, the development of nighttime light imagery began in the 1970s with the Defense Meteorological Satellite Program (DMSP), which was carried out by the Operational Linescan System (OLS). This system was designed to enable effective weather forecasting using the night imaging capability of its embedded sensors. These sensors can effectively capture the weak moonlight reflected from clouds

and thus obtain the cloud cover distribution at night. However, it was inadvertently discovered that in the absence of clouds, these images can clearly capture light emitted by human activity on the Earth's surface. This prompted a new field of scientific research based on nighttime light data [3].

The current mainstream nighttime light data originate from the Visible Infrared Imaging Radiometer Suite (VIIRS) Day/Night Band (DNB) night-lights imagery system and the DMSP/OLS [4]. It is also interesting to note that the OLS sensors on DMSP satellites can capture a variety of light spectra of different intensities, such as small residential areas, traffic lights, fires, boat lights, etc. As a result, changes in the intensity of human economic and social activities can be estimated. However, the OLS sensor acquires night-light images with a digital number (DN) range of only 0–63, which leads to the oversaturation of light values in areas with high light levels. In addition, DMSP data are provided by satellites of different ages with different sensors, leading to inconsistent data that require continuity correction. The VIIRS/DNB, which is considered a second-generation night-light imagery system, offers significant improvements in terms of extracted data quality while inheriting the characteristics of DMSP data. Moreover, the spatial resolution of VIIRS/DNB imagery is much better than that of DMSP/OLS data, allowing for more accurate representations of the nighttime lights without oversaturation issues. Many studies have explored techniques for handling these two types of night-light images and rendering them more suitable for practical use [5–7]. Unlike traditional remote sensing imagery, which is commonly used for land feature classification [8–10], the night-light imagery approach is currently widely employed for various applications, including the estimation of gross domestic product [11], populations [12], poverty [13], and carbon emissions [14,15]. Furthermore, it has been actively used to map urbanization processes [16–18], monitor disasters [19], monitor armed conflicts [20,21], examine ecological light pollution [22], map fires [23], monitor fisheries [24], and monitor power outages [25] and grid reliability [26]. Night-light data have been also employed to determine electrification processes [27–29].

Night-light images can reflect the density and usage of lighting infrastructure. Therefore, they can also be used as an index of electricity consumption in an area, which is a subject that has been studied extensively. Indeed, linear correlations between electricity consumption and light intensity (from DMSP/OLS night-light images) have been reported in a dozen Asian countries, providing preliminary evidence of the feasibility of modelling electricity consumption based on night-light data [30]. Chand et al., simulated both the spatial and temporal patterns of total electricity consumption in India from 1993 to 2002 based on the correlation between light intensity from DMSP/OLS night-light images and electricity consumption [31]. Researchers using night-light imagery for electricity consumption estimates often construct one-dimensional regression models, such as linear regression, power function regression, or exponential regression, to relate electricity consumption to the total night-light value of images. A researcher will choose the regression model with the highest  $R^2$ -value to estimate electricity consumption. Early studies have tended to use DMSP/OLS night-light imagery due to its availability, which covers the time period of 1992–2013. With the advent of better quality VIIRS/DNB night-light images in 2012, researchers have increasingly used these images for their studies. In another interesting work, Shi et al., studied the boundaries and electricity consumption of 12 cities in China using VIIRS/DNB night-light data. The results revealed that the VIIRS/DNB method is more accurate than the DMSP/OLS approach for estimating the total electricity consumption, based on simulations [32]. It has been also been found that VIIRS/DNB images, with their higher quality data, are more accurate in simulating electricity consumption [33,34]. Both DMSP/OLS and VIIRS/DNB night-light images require denoising, the quality of which has a direct impact on subsequent analyses. However, previous simulations of electricity consumption based on night-light data have mainly focused on areas with low cloudiness. Associated denoising methods also focus on less cloudy areas, whereas few studies have been conducted on cloudy areas. In the denoising of cloudy areas, common denoising

methods can mask useful information, such that the denoised images do not reflect the true night-light conditions.

In response to the various problems encountered in previous studies, this study proposes a new method for denoising and making annual image syntheses of night-light images in cloudy areas. The country of Cambodia is used as an example, and VIIRS/DNB night-light images with high accuracy were used to simulate electricity consumption. Multiple one-dimensional regression models were used to explore the relationship between annual electricity consumption and total night-light values in Cambodia. The best model was used to estimate the annual electricity consumption in Cambodia and the changes in its spatial distribution pattern. Hence, a new method of annual electricity consumption estimation and spatial distribution modelling in Cambodia is provided. This work also provides a methodological reference for using night-light imagery to estimate annual electricity consumption in cloudy areas. The results are anticipated to contribute to the planning of electricity infrastructure in Cambodia and the realisation of SDG7.

## 2. Study Area and Materials

### 2.1. Study Area

Cambodia is located in the South Central Peninsula of Southeast Asia. The Electricity Authority of Cambodia (EAC) and the Ministry of Mines and Energy of Cambodia (MME) manage its electricity development. In the 21st century, Cambodia entered a phase of rapid development; the installed power plant capacity increased from 231 MW in 2005 to 3028 MW in 2019, whereas the electricity supply increased from 977 GWh in 2005 to 2015 GWh in 2019, increases of 14.5- and 12-fold, respectively. Indeed, Cambodia's electricity consumption is growing at a much faster rate than that of the rest of the world. This increased access to electricity has significantly contributed to the rapid growth in total electricity consumption. Additionally, there are a large number of areas with lighting, leading to significant growth in both electricity consumption and demand. According to the EAC, unlike most developed countries where the majority of electricity is consumed by industry, Cambodia's significant increase in electricity consumption is related to the provision of lighting in areas where it was previously extremely scarce. This makes it certain that Cambodia's rapid growth in electricity consumption will be well reflected in the total nighttime light data of nighttime images.

### 2.2. Materials

#### 2.2.1. Cambodian Electricity Consumption Data

Data on electricity consumption in Cambodia from 2005 to 2019 were obtained from the EAC (Table 1). The EAC is authorised by the Royal Government to act as an autonomous body for regulating electricity services and managing the relationship between electricity transmission, receipt, and use. The EAC is also responsible for controlling electricity services and electricity use throughout the country. In addition, it has the duty to issue, modify, revoke, or suspend licences for electricity services, approve tariffs, issue regulations for control, impose fines, and settle disputes relating to electricity services and use.

**Table 1.** Electricity consumption in Cambodia, 2012–2019.

Year	Electricity Consumption (GWh)
2012	3527
2013	4051
2014	4713
2015	5990
2016	7175
2017	8073
2018	9739
2019	12,015

### 2.2.2. VIIRS/DNB Night-Light Images

Due to having higher image quality and spatial resolution than other systems, VIIRS/DNB nighttime light data are more accurate for use in electricity consumption simulations. A total of 92 monthly nighttime light images were used in this work, which were published by the Payne Institute for Public Policy from April 2012 to December 2019. The National Polar-orbiting Partnership satellite was launched in October 2011, with the DNB band used to detect nighttime lights in the wavelength range of 0.5–0.9  $\mu\text{m}$  at a spatial resolution of 750 m and 14-bit spectral resolution with in-orbit radiometric calibration. The Group on Earth Observations (GEO) uses nighttime data from the Visible Infrared Imaging Radiometer Suite (VIIRS) day/night band (DNB) to produce monthly average synthetic data. Prior to averaging, the cloud coverage was determined using the VIIRS Cloud Mask product (VCM), while the DNB data were filtered to exclude data affected by stray light, lightning, lunar illumination, and cloud cover. Moreover, the data near the edges of the strips were excluded from the averaging calculations. The product is offered in GeoTIFF format in sets of six tiles. More specifically, the tiles are cut at the equator and each spans 120 degrees of latitude. The current monthly composite image is filtered to screen out light from auroras, fires, boats, and other temporary sources, and has not been background denoised. However, the incorporation of layers of annual composites can eliminate the temporary light and background (non-light) values, and the first version of annual images includes only two years: 2015 and 2016.

## 3. Methods

Cambodian electricity consumption data were used in this work in conjunction with VIIRS/DNB night-light remote sensing data. The data were first pre-processed by cropping the downloaded monthly VIIRS/DNB images from 2012 to 2019 to obtain images of the Cambodian region. Afterwards, they were denoised and projected as Albers equivalent cone projections and resampled to a 500 m spatial resolution. Then, three different methods were used—the annual average method, annual cloud-free average method, and month-specific substitution method—to obtain average night-light remote sensing images of Cambodia for each year from 2012 to 2019. Finally, electricity consumption data for Cambodia from 2012 to 2019 were fitted by functional models of total night-light data obtained from each of the three methods to determine the best model. This provided estimates of Cambodia's electricity consumption and its spatial distribution. A flowchart of the research process is presented in Figure 1.

### 3.1. Data Pre-Processing

The VIIRS/DNB is a primary data product in a split format that requires extensive pre-processing, such as cropping, reprojection, and denoising, to obtain images of the desired areas. A total of 92 monthly nighttime images from April 2012 to December 2019 were masked using a vector of the Cambodian border to obtain VIIRS/DNB nighttime images of the Cambodian region. To ensure minimal areal distortion, the data were projected as Albers' cone of equivalence; the area of the region is proportional to the area of the same region on Earth, while the area of the Cambodian region is less distorted. Finally, the monthly night-light images were resampled to a 500 m spatial resolution.

Since the acquired VIIRS/DNB night-light images had not yet been stripped of auroras, fires, other transient light sources, and background noise, a large number of negative and very high values existed in the night-light images. Theoretically, it is not possible for image elements to have negative DN values. Nevertheless, negative DN values were caused by background noise and outliers during data processing. The maximum light value in an image should not be greater than the highest light value in the most developed area of the image. DN values greater than the highest light value in the developed area are called extreme values, which mainly originate from fires and data outliers. To reduce the impact of noise on image elements, the images needed to be denoised. The three most widely used methods for denoising VIIRS/DNB luminous images are: (1) stable nighttime

lights extracted from VIIRS/DNB data using non-zero DMSP/OLS data as a mask [35]; (2) selection of area-specific thresholds as maximum and minimum light thresholds as masks for rejecting background noise [36]; (3) denoising night-light images by enforcing the neighbourhood algorithm [32,37]. All these methods can significantly enhance the quality of images by removing some of the noise and light from auroras, fires, and certain ephemeral light sources. Although the first denoising method can remove noise, it also removes much usable night-light information. This method is more suitable for studies of short time series and regions with little change in the size of the energised area. However, from 2012 to 2019, electricity consumption in Cambodia increased at a faster rate than before and a large number of un electrified areas became connected to electricity. For this reason, we can draw the conclusion that this method is not suitable for denoising long time series of the Cambodian region. Furthermore, since Cambodia’s night-light images are seriously affected by cloud, the neighbourhood algorithm is also unsuitable. Accordingly, the threshold method was selected for image denoising in the present study. Phnom Penh is the most developed region in Cambodia, so was used to establish a theoretical maximum value of the image element DN for the 2012–2019 night-light images. Image element DN values in the annual average images that were greater than the theoretical maximum were replaced by the maximum value, while negative values were replaced with zero-values. This completed the first denoising process for the 2012–2019 night-light images.

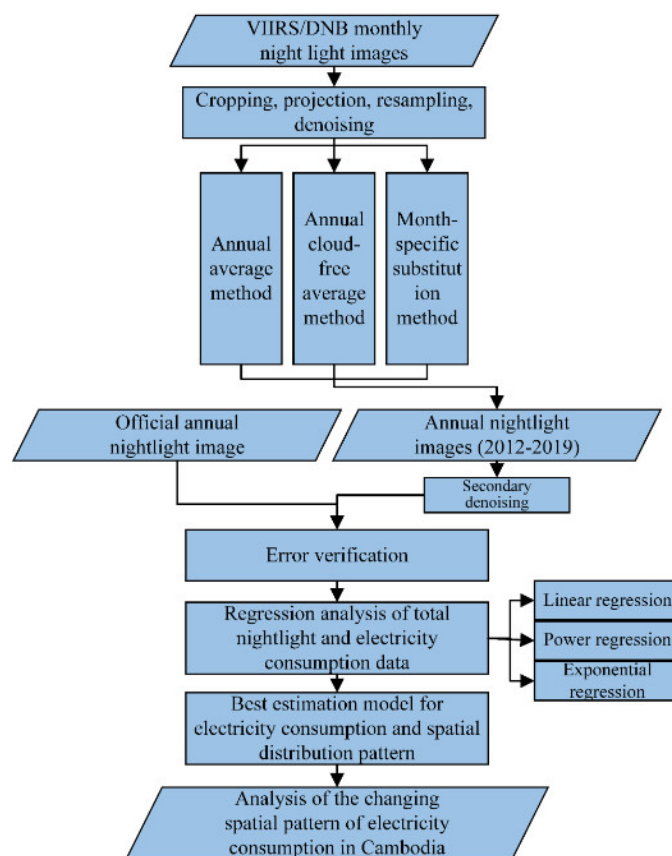


Figure 1. Flowchart of the research process used in the present study.

The threshold denoising procedure removes both negative and extreme values from images; however, it is difficult to remove other sources of noise. The denoising method employed in this work is based on Cao et al.’s continuity correction method for night-light images in different years [38]. (1) More specifically, when  $DN = 0$  in an image of the subsequent year, then the  $DN$  at the same position in the previous year’s image should also equal 0. (2) On the other hand, when the  $DN$  value of an image element in a later year’s

image is not equal to 0, the  $DN$  in the previous year’s image should be no greater than that. The formula for this denoising method is as follows:

$$DN_{(n,i)} = \begin{cases} 0 & DN_{(n+1,i)} = 0 \\ DN_{(n+1,i)} & DN_{(n+1,i)} > 0 \text{ and } DN_{(n,i)} > DN_{(n+1,i)} \\ DN_{(n,i)} & n = 2019 \end{cases} \quad (1)$$

where  $DN_{(n,i)}$  and  $DN_{(n+1,i)}$  denote the  $DN$  values of image  $i$  in years  $n$  and  $n + 1$ , respectively. The extracted night-light image, from which the negative and extreme values have been removed, is denoised a second time using this formula. Figure 2 gives an example dataset showing the changes in the raster values of the night-light images for years  $n - 1$ ,  $n$  and  $n + 1$  before and after denoising.

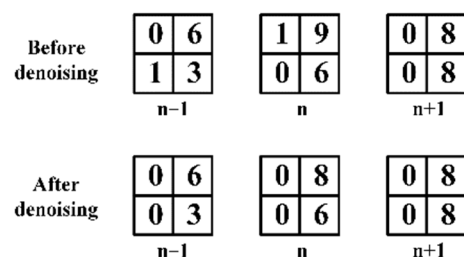


**Figure 2.** Examples of changes in night-light image raster data for different years before and after denoising (years  $n - 1$ ,  $n$  and  $n + 1$ ).

### 3.2. Three Methods for Obtaining Annual Night-Light Images

To synthesise a suitable annual night-light image for the Cambodian region, which will be heavily influenced by cloud cover, three methods were used: annual average, annual cloud-free average, and month-specific substitution. In a night sky without clouds, light emanating from the surface can be captured by satellites; if there are clouds in the atmosphere, satellites cannot capture nighttime lights beneath them. Daily data products based on VIIRS/DNB night-light imagery cannot be used to estimate electricity consumption, as they are heavily influenced by cloud cover. Monthly data products from VIIRS/DNB night-light imagery are synthesised from the daily data products and, when an area is obscured by clouds, that day’s data are replaced by the non-obscured days for that month. With this process, unobstructed monthly night-light images are available for most of the world; however, in low latitudes like the Cambodian region, there are still many months of the year when unobstructed monthly images are not available. In this study, months that were unaffected by cloud cover after daily data synthesis are called *cloud-free months*.

(1) Annual average method

Annual night-light images were obtained by averaging the night-light values of the twelve monthly images of the year, regardless of whether they were affected by cloud.

(2) Annual cloud-free average method

Cambodia experiences distinct dry and rainy seasons, such that night-light images are often heavily influenced by cloud cover in the rainy season. Using the annual cloud-free average method, the cloud-influenced months in Table 2 were excluded and the night-light images from non-cloud-influenced months were averaged to obtain annual night-light images.

**Table 2.** Cloud-free months in night-light images of Cambodia, 2012–2019.

Year	Cloud-Free Months
2012	12
2013	1, 2, 3, 4, 10, 11, 12
2014	1, 2, 3, 11, 12
2015	1, 2, 3, 4, 5, 9, 11, 12
2016	1, 2, 3, 4, 5, 11, 12
2017	1, 2, 3, 4, 12
2018	1, 2, 3, 4, 10, 11, 12
2019	1, 2, 3, 4, 10, 11, 12

(3) Month-specific substitution method

December is part of the dry season in Cambodia and is the month least affected by cloud. As a result, the December night-light images for each year from 2012 to 2019 are not affected by cloud cover and are the most stable. Thus, this method used December night-light images as annual night-light images.

3.3. Coupled Model of Electricity Consumption and Total Night-Light Value

Denosed night-light images only contain electrical illumination, e.g., from streetlights. Using Cambodia’s electricity consumption from 2012 to 2019 as the independent variable and the total night-light value of annual night-light images data as the dependent variable, several one-dimensional regression models were established based on linear, power, and exponential functions. The regression models for this study were obtained via curve fitting using the *ordinary least squares* (OLS) and *maximum likelihood estimation* (MLE) methods [39]. Linear optimization problems like linear regression models are obtained by OLS, and non-linear optimization problems like exponential models are obtained by MLE. The equations for these three regression models are shown in Table 3.

**Table 3.** The three regression models used in this study.

Regression Models	Mathematical Equation
Linear	$y = ax + b$
Power	$y = ax^b$
Exponential	$y = ae^{bx}$

In the mathematical equation,  $x$  represents electricity consumption,  $y$  represents the total night-light value,  $e$  is a natural constant,  $a$  and  $b$  are the derived coefficients after performing the OLS regression.

The models were evaluated in terms of the adjusted coefficient of determination ( $\text{adj-}R^2$ ) and its significance ( $p$ ). In regression analysis, the coefficient of determination ( $R^2$ ) is used to determine the explanatory power of a model. This process measures the proportion of variation in the dependent variable that can be explained by the independent variable. The  $\text{adj-}R^2$  can eliminate the effect of variation in the number of independent variables and is more appropriate for judging the merits of a regression model than  $R^2$ ; higher  $\text{adj-}R^2$  values indicate a better model. Significant differences in the regression analysis are an evaluation of the variability of the data. Significant differences are usually expressed as  $p > 0.05$  for non-significant differences,  $0.01 < p < 0.05$  for significant differences, and  $p < 0.01$  for very significant differences. In regression analysis, a regression model is often considered valid when  $p < 0.05$ . The smaller the  $p$ -value, the higher the correlation between the two sets of data and the better the regression model.

3.4. Error Analysis

Error analysis of the annual night-light images of Cambodia, pre-processed by denoising and other means, was conducted using version 1 of the 2015 Nightlight Image of the

Year from the Payne Institute. This image has noise removed, including from auroras, fires, ships, and other temporary light sources. The results obtained in this work were compared with the total night-light values of the official processed data by using the relative error (*RE*) to measure the quality of image processing, according to the following equation:

$$RE = |S_p - S_a| \div S_p \times 100\% \tag{2}$$

where  $S_p$  denotes the total night-light value of the 2015 Cambodian regional image provided by the Payne Institute and  $S_a$  denotes that of the 2015 Cambodian regional images processed by the present study. The smaller the *RE*, the closer the image is to the Payne Institute’s data and the better the processing quality.

### 4. Results

#### 4.1. Denoised Night-Light Images

After the images were pre-processed using various techniques such as denoising, annual night-light images of Cambodia were obtained. It is interesting to note that the denoising method produced better annual images when both the annual cloud-free averaging and month-specific substitution methods were applied. The annual images obtained by the annual averaging method were affected by cloud cover, causing the final image element DN values to be greatly distorted. Examples of the final images corrected by the three methods are shown in Figures 3–5.

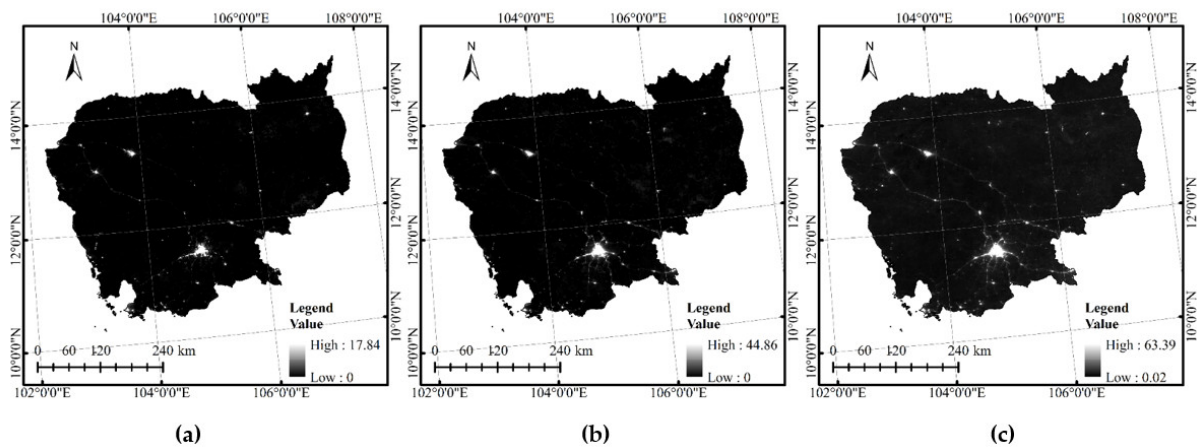


Figure 3. Annual night-light images of Cambodia obtained by the annual averaging method for years (a) 2012, (b) 2015, and (c) 2018.

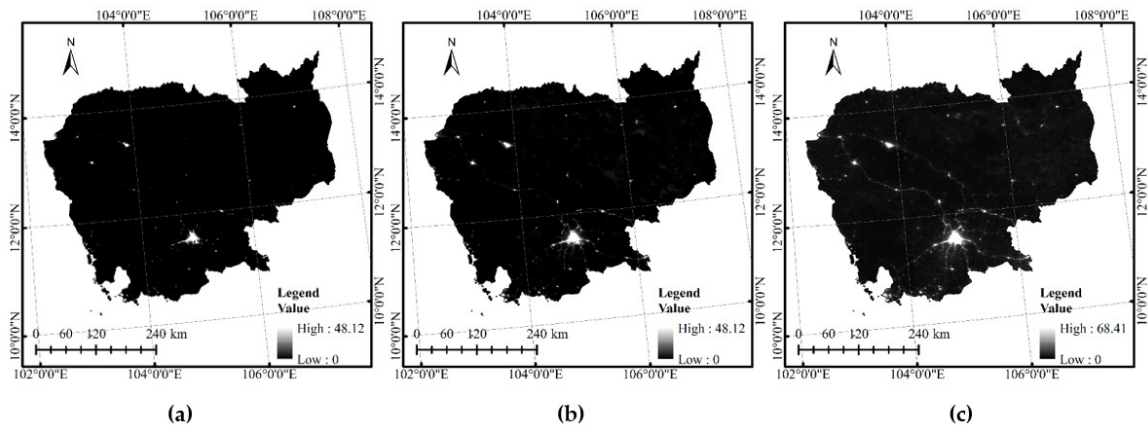
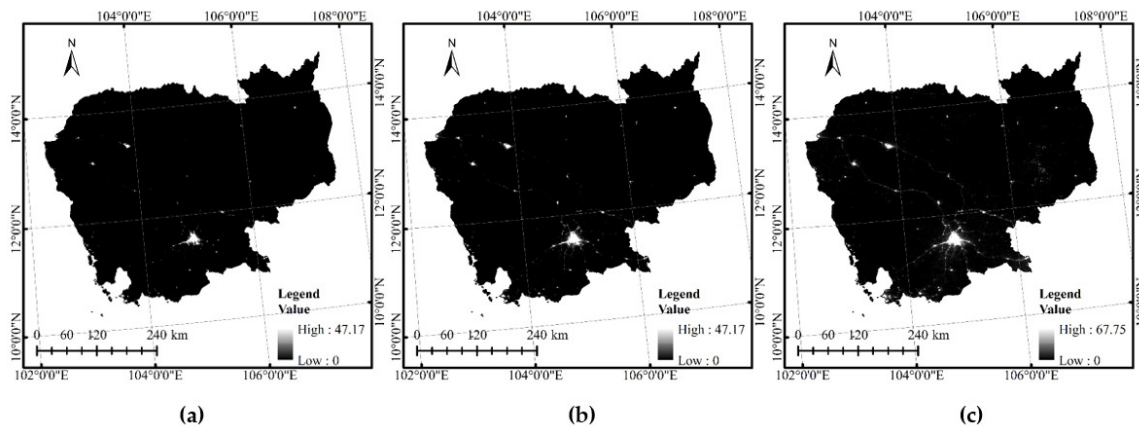


Figure 4. Annual night-light images of Cambodia obtained by cloud-free averaging throughout the years of (a) 2012, (b) 2015, and (c) 2018.



**Figure 5.** Annual night-light images of Cambodia obtained by month-specific substitution for the years (a) 2012, (b) 2015, and (c) 2018.

In this work, the total night-light values of the images obtained using the three different processing methods were counted. The different methods produced similar total night-light values in some years. The overall night-light value for Cambodia is increasing, suggesting that the country’s electricity supply and national access rate are increasing. The specific data are shown in Table 4.

**Table 4.** Total night-light values of annual images obtained by different processing methods.

Year	Annual Average	Annual Cloud-Free Averaging	Month-Specific Substitution
2012	6103.49	11,381.88	10,999.01
2013	15,477.79	15,717.58	13,458.87
2014	20,513.02	17,792.10	16,456.33
2015	26,199.31	27,151.61	19,274.36
2016	29,259.82	31,096.87	23,261.00
2017	119,668.83	115,621.28	44,376.24
2018	125,776.75	124,356.13	54,352.43
2019	149,365.57	142,979.22	88,756.83

**4.2. Coupled Model of Electricity Consumption and Total Night-Light Values in Cambodia**

Electricity consumption from 2012 to 2019 was used as the independent variable and the total night-light values as the dependent variable to construct three regression models using linear, power, and exponential functions. Tables 5–7 show the results, where  $x$  represents electricity consumption,  $y$  represents the total night-light value, and  $e$  is a natural constant in the regression equation. The higher the  $adj-R^2$ -value and the lower the  $p$ -value, the more accurate the model. Normally,  $p$ -values  $> 0.05$  indicate that the regression does not pass the significance test. Tables 5–7 reveal that the  $p$ -values of the nine regression equations obtained in this study were all less than 0.01. Therefore, all these models passed the significance test. The  $adj-R^2$ -values of all these equations are greater than 0.83, indicating a high correlation between the total night-light value and the electricity consumption data. The differences in the  $adj-R^2$ -value across models reflect the quality of the different models and the annual night-light images synthesis methods in Cambodia, as discussed in Section 5.1. The  $a$ -values for the three linear regression models in Tables 5–7 are 18.609, 17.716, and 8.802, respectively. A positive  $a$ -value indicates that the total night-light value increases as electricity consumption increases. The  $b$  values for all three linear models are negative, indicating that the total night-light value is only greater than 0 when the electricity consumption is multiplied by the  $a$  value greater than the  $b$  value. The  $a$  and  $b$  values for the power function regression model and the exponential function regression model in Tables 5–7 are greater than zero, indicating that the total night-light value increases as electricity consumption increases. The total night-light value is 0 for a power function regression model with electricity consumption of 0. The total night-light

value is equal to  $a$  for an exponential regression model with electricity consumption of 0. In fact, the total night-light value of night-light images is often greater than zero in areas where there is no electricity consumption. This suggests that the exponential function regression model is more appropriate for electricity consumption simulation.

**Table 5.** Modelling results for annual night-light data obtained by the annual average method.

Function	Regression Equation	Adj- $R^2$	$p$
Linear	$y = 18.609x - 67,046.725$	0.840	0.001
Power	$y = (7.627 \times 10^{-6})x^{2.5451}$	0.886	0.000
Exponential	$y = 2983.4e^{0.0004x}$	0.835	0.001

**Table 6.** Modelling results for annual night-light data obtained by the annual cloud-free average method.

Function	Regression Equation	Adj- $R^2$	$p$
Linear	$y = 17.716x - 61,658.739$	0.839	0.001
Power	$y = (9.702 \times 10^{-5})x^{2.262}$	0.890	0.000
Exponential	$y = 4057.7e^{0.0003x}$	0.871	0.000

**Table 7.** Modelling results for annual night-light data obtained by the month-specific substitution method.

Function	Regression Equation	Adj- $R^2$	$p$
Linear	$y = 8.802x - 26,956.863$	0.908	0.000
Power	$y = (0.0122)x^{1.6652}$	0.936	0.000
Exponential	$y = 4780.6e^{0.0002x}$	0.967	0.000

The total night-light values for Cambodia obtained by the annual average method were fitted to the electricity consumption data using the three regression models. The exponential model produced the smallest adj- $R^2$ -value, with the linear model being the next best and the power model being the best (Table 5).

Using annual cloud-free average data, the linear regression model had the smallest adj- $R^2$ -value, with the exponential model being the next best and the power model being the best. The results are shown in Table 6.

Next, models were constructed using the data processed by the month-specific substitution method. The linear model had the lowest adj- $R^2$ -value, the power model was second-best, and the exponential model was the best (Table 7).

### 4.3. Error Analysis

The annual night-light data obtained by the three methods were compared with the total night-light values of the officially published 2015 night-light images. The  $RE$ -values were used as a measure of error and were 15.75%, 19.96%, and 14.83% for the annual average, annual cloud-free average, and month-specific substitution methods, respectively (lower values are better).

## 5. Discussion

### 5.1. Analysis of Annual Images Synthesised by Different Methods and Modelling Results

In this work, night-light images of Cambodia from 2012 to 2019 were obtained by processing with three methods. The annual night-light images obtained by the annual average method were heavily influenced by cloud cover and, theoretically, were the least accurate. Although cloud-free months were removed in the annual cloud-free average method, these months varied interannually, which could influence the comparability of images from one year to another. Furthermore, the December night-light images from different years were slightly affected by cloud cover. By taking into account that December is the last month of the year, the annual images obtained by month-specific substitution method possess better continuity between years and, theoretically, produce the best modelling results. Ranking

the quality of different models according to the magnitude of adj- $R^2$ -value and significance, the results confirm these suspicions. The only exception was with the month-specific substitution method, where the linear model had a slightly higher adj- $R^2$ -value than that of the cloud-free averaging method. The adj- $R^2$  values and significance rankings for the other regression methods show that the annual average method < annual cloud-free average method < month-specific substitution method. This conclusion suggests that the three annual night-light image synthesis methods should be ranked as follows: annual average method < annual cloud-free average method < month-specific substitution method. The results of the regression models are shown in Table 8.

**Table 8.** Results of the regression models of total night-light data vs. electricity consumption.

Image Composition Method	Linear Model		Exponential Model		Power Model	
	Adj- $R^2$	$p$	Adj- $R^2$	$p$	Adj- $R^2$	$p$
Annual average	0.840	0.001	0.835	0.001	0.886	0.000
Annual cloud-free average	0.839	0.001	0.871	0.000	0.890	0.000
Month-specific substitution	0.908	0.000	0.967	0.000	0.936	0.000

Table 8 indicates that when using data processed by the annual average method, the quality of the regression models is ranked exponential < linear < power. Using data processed by the annual cloud-free average method, the model accuracy is ranked linear < exponential < power. Using data processed by the month-specific substitution method, the model accuracy is ranked linear < power < exponential. The overall quality of the annual images synthesized by different methods is annual average < annual cloud-free average < month-specific substitution. The exponential model was ranked third, second, and first using data from the annual averaging, annual cloud-free averaging, and month-specific substitution methods, respectively. This suggests that as the annual night-light image synthesis method becomes more reasonable, an exponential regression model provides a better fit. Therefore, the relationship between electricity consumption and total night-light values in Cambodia is best expressed using an exponential regression model.

### 5.2. Estimated Annual Electricity Consumption in Cambodia

This study demonstrates a strong correlation between electricity consumption and total annual night-light values in Cambodia, with an adj- $R^2$  of 0.97 using month-specific substitution data. This effect clearly demonstrates the feasibility of using night-light data to estimate annual electricity consumption. With the estimated electricity consumption in Cambodia from 2012 to 2019 using the exponential regression model, Table 9 was obtained.

**Table 9.** Estimated annual electricity consumption in Cambodia, 2012–2019.

Year	Electricity Consumption (GWh)	RE
2012	3472.81	1.54%
2013	4266.32	5.32%
2014	5056.83	7.30%
2015	5678.27	5.20%
2016	6417.40	10.56%
2017	8956.86	10.95%
2018	9754.11	0.16%
2019	11,682.16	2.78%

Table 9 shows that electricity consumption in Cambodia from 2012 to 2019 estimated from night-light data had RE-values of 0.16–10.95% with a mean of 5.47%, which is a good overall result.

Electricity consumption and demand are influenced by several factors, which is a focus of research. Recent research on national electricity consumption and electricity demand prediction has focused on the development of complex models. Rivera-Gonzalez et al.,

modelled Ecuador's electricity consumption and demand until 2040 using the Long-range Energy Alternatives Planning (LEAP) system [40]. Pakistan's electricity consumption and demand were investigated by Perwez et al., using the LEAP system [41]. Shah et al., forecasted day-ahead electricity demand with nonparametric functional models [42] and subsequently used a component-estimation technique to forecast short-term electricity demand [43]. Other researchers have recently used deep learning for energy time series forecasting [44]. With the development of night-light remote sensing technology, research on electricity consumption based on night-light data is gradually increasing. Unlike data obtained from traditional surveys, satellite imagery records data that are more objective, have wider coverage, and cost less to obtain. The use of night-light images for electricity consumption prediction only requires a simple one-dimensional regression model. The required data are easy to obtain, and the predictive accuracy is high, providing a novel and simple method of electricity consumption prediction.

### 5.3. Changing Spatial Patterns of Electricity Consumption in Cambodia

Timely and accurate access to data on the spatial distribution of electricity consumption is essential in the construction of electrical infrastructure and for assessing the achievement of SDG7. Total night-light data from 2012 to 2019 were used to obtain the spatial pattern of electricity consumption in Cambodia at a 500 m resolution (Figure 6 shows three years as examples).

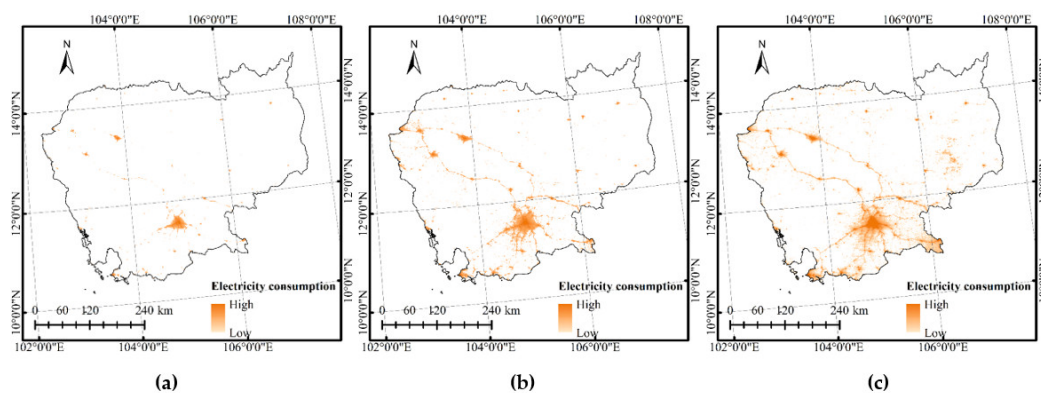


**Figure 6.** Spatial distributions of electricity consumption in Cambodia in years (a) 2012, (b) 2015, and (c) 2018.

The analysis of the spatial pattern of electricity consumption in Cambodia discloses that in 2012, electricity was mainly consumed in the capital city of Phnom Penh, the southwestern port city of Sihanoukville, and the northwestern cities of Battambang and Siem Reap. Interestingly, these four cities are the most economically developed regions in Cambodia and have the highest electricity consumption. From 2012 to 2019, the electricity consumption in Cambodia has been spreading outwards from these four cities, demonstrating the phenomenon of urban sprawl. The rapid increases in electricity consumption in the vicinity of the two main transport routes along the western part of Cambodia indicate that transport has made a huge boost to Cambodia's development. Additionally, the country's electricity coverage has improved considerably in recent years, with its electricity consumption slowly spreading from the major cities to the vast rural areas. The most rapid growth in electricity consumption has occurred in the southwestern port city of Sihanoukville and the southeastern province of Svay Rieng, which are inextricably linked to Cambodia's national development strategy and Chinese investment.

### 5.4. Limitations Analysis

(1) The proposed denoising method required high-quality night-light images from 2019. If the quality of the images from 2019 was poor, the overall denoising effect could be

poor. In addition, recent years are not as good at denoising as previous years, e.g., 2017 is better at denoising than 2018 and 2018 is better than 2019.

(2) The data used in this work were only available until 2019, so the latest years were not included.

(3) As Cambodia is located in a cloudy region at low latitudes, many of its daily night-light images are heavily obscured by clouds and were unusable. Meanwhile, monthly images are only affected by cloud for some months of the year. Only December was cloud-free in all years. This means that the estimation of electricity consumption and its spatial distribution were only possible on an annual scale and not on daily or monthly scales.

(4) When using night-light images to estimate electricity consumption and its spatial pattern, it is particularly important to denoise the images, as this estimation method is ineffective if the noise cannot be effectively removed. Moreover, a set of electricity consumption data corresponding to the year of the night-light images is required for building regression models.

## 6. Conclusions

A novel method is proposed for denoising night-light images of cloudy areas. It was used to denoise annual night-light image data from Cambodia that were synthesised by three methods. The *RE* value of the annual luminous image synthesized by the month-specific substitution method and processed by this denoising method was 14.83%, which is considered a relatively good denoising effect. The total night-light values were then related to electricity consumption data using several functional models. The results show that the best regression model was the exponential model. The three methods of the annual image composition in Cambodia are ranked in the order of merit of annual average method < annual cloud-free average method < month-specific substitution method. The use of the exponential model to forecast electricity consumption and its spatial patterns in Cambodia showed that the model performed well, with an average *RE* of 5.47% for consumption forecasts. A simulation of the spatial distribution of electricity consumption showed that from 2012 to 2019, Cambodia's electricity consumption spread outwards along main transport routes from the four major cities to a large number of rural areas. Many unelectrified areas were connected to electricity and the four most economically developed cities in the country.

This study shows that night-light images in cloudy areas can still be used to simulate electricity consumption and its spatial distribution with high accuracy if denoising is applied. The results of this study will contribute to the planning of electricity infrastructure development in Cambodia and the measurement of the achievement of SDG7.

**Author Contributions:** Methodology, X.G. and M.W.; formal analysis, X.G.; data curation, J.G. and L.H.; writing—original draft preparation, X.G., J.G. and M.W.; writing—review and editing, X.G., L.H. and M.W.; supervision, Z.N. and F.C.; project administration, M.W. and Z.N.; funding acquisition, Z.N. and F.C. All authors have read and agreed to the published version of the manuscript.

**Funding:** This research was funded by the Strategic Priority Research Program of the Chinese Academy of Science, grant number XDA19030304.

**Institutional Review Board Statement:** Not applicable.

**Informed Consent Statement:** Not applicable.

**Data Availability Statement:** The data presented in this study are available upon request from the corresponding author.

**Conflicts of Interest:** The authors declare no conflict of interest.

## References

1. Rajkumari, L. Relation between electricity consumption and economic growth in Karnataka, India: An aggregate and sector-wise analysis. *Electr. J.* **2020**, *33*, 106768. [[CrossRef](#)]
2. Rao, N.D. Does (better) electricity supply increase household enterprise income in India? *Energy Policy* **2013**, *57*, 532–541. [[CrossRef](#)]
3. Croft, T.A. Nighttime images of the earth from space. *Sci. Am.* **1978**, *239*, 86–101. [[CrossRef](#)]
4. Levin, N.; Kyba, C.C.M.; Zhang, Q.L.; de Miguel, A.S.; Roman, M.O.; Li, X.; Portnov, B.A.; Molthan, A.L.; Jechow, A.; Miller, S.D.; et al. Remote sensing of night lights: A review and an outlook for the future. *Remote Sens. Environ.* **2020**, *237*, 111443. [[CrossRef](#)]
5. Bian, J.H.; Li, A.N.; Huang, C.Q.; Zhang, R.; Zhan, X.W. A self-adaptive approach for producing clear-sky composites from VIIRS surface reflectance datasets. *Isprs. J. Photogramm. Remote Sens.* **2018**, *144*, 189–201. [[CrossRef](#)]
6. Chen, Z.Q.; Yu, B.L.; Yang, C.S.; Zhou, Y.Y.; Yao, S.J.; Qian, X.J.; Wang, C.X.; Wu, B.; Wu, J.P. An extended time series (2000–2018) of global NPP-VIIRS-like nighttime light data from a cross-sensor calibration. *Earth Syst. Sci. Data* **2021**, *13*, 889–906. [[CrossRef](#)]
7. Li, X.C.; Zhou, Y.Y.; Zhao, M.; Zhao, X. A harmonized global nighttime light dataset 1992–2018. *Sci. Data* **2020**, *7*, 168. [[CrossRef](#)]
8. Tian, H.F.; Wang, Y.J.; Chen, T.; Zhang, L.J.; Qin, Y.C. Early-Season Mapping of Winter Crops Using Sentinel-2 Optical Imagery. *Remote Sens.* **2021**, *13*, 3822. [[CrossRef](#)]
9. Tian, H.F.; Qin, Y.C.; Niu, Z.; Wang, L.; Ge, S.S. Summer Maize Mapping by Compositing Time Series Sentinel-1A Imagery Based on Crop Growth Cycles. *J. Indian Soc. Remote Sens.* **2021**, *49*, 2863–2874. [[CrossRef](#)]
10. Tian, H.; Chen, T.; Li, Q.; Mei, Q.; Wang, S.; Yang, M.; Wang, Y.; Qin, Y. A Novel Spectral Index for Automatic Canola Mapping by Using Sentinel-2 Imagery. *Remote Sens.* **2022**, *14*, 1113. [[CrossRef](#)]
11. Elvidge, C.D.; Baugh, K.E.; Kihn, E.A.; Kroehl, H.W.; Davis, E.R.; Davis, C.W. Relation between satellite observed visible-near infrared emissions, population, economic activity and electric power consumption. *Int. J. Remote Sens.* **1997**, *18*, 1373–1379. [[CrossRef](#)]
12. Lo, C.P. Modeling the population of China using DMSP operational linescan system nighttime data. *Photogramm. Eng. Remote Sens.* **2001**, *67*, 1037–1047.
13. Jean, N.; Burke, M.; Xie, M.; Davis, W.M.; Ermon, S. Combining satellite imagery and machine learning to predict poverty. *Science* **2016**, *353*, 790–794. [[CrossRef](#)]
14. Ghosh, T.; Elvidge, C.D.; Sutton, P.C.; Baugh, K.E.; Ziskin, D.; Tuttle, B.T. Creating a Global Grid of Distributed Fossil Fuel CO<sub>2</sub> Emissions from Nighttime Satellite Imagery. *Energies* **2010**, *3*, 1895–1913. [[CrossRef](#)]
15. Ou, J.P.; Liu, X.P.; Li, X.; Li, M.F.; Li, W.K. Evaluation of NPP-VIIRS Nighttime Light Data for Mapping Global Fossil Fuel Combustion CO<sub>2</sub> Emissions: A Comparison with DMSP-OLS Nighttime Light Data. *PLoS ONE* **2015**, *10*, e0138310. [[CrossRef](#)] [[PubMed](#)]
16. Zhou, Y.Y.; Li, X.C.; Asrar, G.R.; Smith, S.J.; Imhoff, M. A global record of annual urban dynamics (1992–2013) from nighttime lights. *Remote Sens. Environ.* **2018**, *219*, 206–220. [[CrossRef](#)]
17. Zhu, Z.; Zhou, Y.Y.; Seto, K.C.; Stokes, E.C.; Deng, C.B.; Pickett, S.T.A.; Taubenbock, H. Understanding an urbanizing planet: Strategic directions for remote sensing. *Remote Sens. Environ.* **2019**, *228*, 164–182. [[CrossRef](#)]
18. Zhou, Y.Y.; Smith, S.J.; Elvidge, C.D.; Zhao, K.G.; Thomson, A.; Imhoff, M. A cluster-based method to map urban area from DMSP/OLS nightlights. *Remote Sens. Environ.* **2014**, *147*, 173–185. [[CrossRef](#)]
19. Zhao, X.Z.; Yu, B.L.; Liu, Y.; Yao, S.J.; Lian, T.; Chen, L.J.; Yang, C.S.; Chen, Z.Q.; Wu, J.P. NPP-VIIRS DNB Daily Data in Natural Disaster Assessment: Evidence from Selected Case Studies. *Remote Sens.* **2018**, *10*, 1526. [[CrossRef](#)]
20. Li, X.; Liu, S.S.; Jendryke, M.; Li, D.R.; Wu, C.Q. Night-Time Light Dynamics during the Iraqi Civil War. *Remote Sens.* **2018**, *10*, 858. [[CrossRef](#)]
21. Li, X.; Li, D.; Xu, H.; Wu, C. Intercalibration between DMSP/OLS and VIIRS night-time light images to evaluate city light dynamics of Syria's major human settlement during Syrian Civil War. *Int. J. Remote Sens.* **2017**, *38*, 5934–5951. [[CrossRef](#)]
22. Koen, E.L.; Minnaar, C.; Roever, C.L.; Boyles, J.G. Emerging threat of the 21st century lightscape to global biodiversity. *Glob. Chang. Biol.* **2018**, *24*, 2315–2324. [[CrossRef](#)] [[PubMed](#)]
23. Chand, T.R.K.; Badarinath, K.V.S.; Murthy, M.S.R.; Rajsheshkar, G.; Elvidge, C.D.; Tuttle, B.T. Active forest fire monitoring in ttaranchal state, India using multi-temporal DMSP-OLS and MODIS data. *Int. J. Remote Sens.* **2007**, *28*, 2123–2132. [[CrossRef](#)]
24. Elvidge, C.; Tilottama, G.; Kimberly, B.; Mikhail, Z.; Feng-Chi, H.; Selim, K.N.; Wilmon, P.; Quang, H.B. Rating the Effectiveness of Fishery Closures with Visible Infrared Imaging Radiometer Suite Boat Detection Data. *Front. Mar. Ence.* **2018**, *5*, 132. [[CrossRef](#)]
25. Cole, T.A.; Wanik, D.W.; Molthan, A.L.; Roman, M.O.; Griffin, R.E. Synergistic Use of Nighttime Satellite Data, Electric Utility Infrastructure, and Ambient Population to Improve Power Outage Detections in Urban Areas. *Remote Sens.* **2017**, *9*, 19. [[CrossRef](#)]
26. Shah, Z.; Taneja, J. Poster Abstract: Monitoring Electric Grid Reliability Using Satellite Data. In Proceedings of the 6th ACM International Conference on Systems for Energy-Efficient Buildings, Cities, and Transportation (BuildSys), New York, NY, USA, 13–14 November 2019; pp. 378–379.
27. Falchetta, G.; Pachauri, S.; Parkinson, S.; Byers, E. A high-resolution gridded dataset to assess electrification in sub-Saharan Africa. *Sci. Data* **2019**, *6*, 9. [[CrossRef](#)]
28. Ramdani, F.; Setiani, P. Multiscale assessment of progress of electrification in Indonesia based on brightness level derived from nighttime satellite imagery. *Environ. Monit. Assess.* **2017**, *189*, 15. [[CrossRef](#)]

29. Principe, J.; Takeuchi, W. Supply and Demand Assessment of Solar PV as Off-Grid Option in Asia Pacific Region with Remotely Sensed Data. *Remote Sens.* **2019**, *11*, 21. [[CrossRef](#)]
30. Letu, H.; Hara, M.; Yagi, H.; Tana, G.; Nishio, F. Estimating the energy consumption with nighttime city light from the DMSP/OLS imagery. In Proceedings of the Joint Workshop on Urban Remote Sensing, Shanghai, China, 20–22 May 2009; pp. 1–7.
31. Chand, T.R.K.; Badarinath, K.V.S.; Elvidge, C.D.; Tuttle, B.T. Spatial characterization of electrical power consumption patterns over India using temporal DMSP-OLS night-time satellite data. *Int. J. Remote Sens.* **2009**, *30*, 647–661. [[CrossRef](#)]
32. Shi, K.F.; Yu, B.L.; Huang, Y.X.; Hu, Y.J.; Yin, B.; Chen, Z.Q.; Chen, L.J.; Wu, J.P. Evaluating the Ability of NPP-VIIRS Nighttime Light Data to Estimate the Gross Domestic Product and the Electric Power Consumption of China at Multiple Scales: A Comparison with DMSP-OLS Data. *Remote Sens.* **2014**, *6*, 1705–1724. [[CrossRef](#)]
33. Qiu, Y.Q.; Xue, X.Y.; Han, W.J.; Chen, X.L.; Xi, L.I. Comparison of Radiation Intensity and Estimation of Electric Power Consumption between DMSP/OLS and VIIRS Nighttime Light Images. *J. Appl. Sci.* **2019**, *37*, 99–111.
34. Wei, J.; He, G.; Liu, H. Modelling regional socio-economic parameters based on comparison of NPP/VIIRS and DMSP/OLS nighttime light imagery. *Remote Sens. Inf.* **2016**, *31*, 28–34.
35. Feng, L.; Aixia, W.; Xiaonan, M.; Guangtong, S. An approach of GDP spatialization in Hebei province using NPP-VIIRS nighttime light data. *J. Xinyang Norm. Univ.* **2016**, *29*, 152–156.
36. Zhong, L.; Liu, X.; Yang, P. Method for SNPP-VIIRS nighttime lights images denoising. *Bull. Surv. Mapp.* **2019**, *3*, 21–26. [[CrossRef](#)]
37. Hu, Y.; Zhao, G.; Zhang, Q. Spatial distribution of population data based on nighttime light and LUC data in the Sichuan-Chongqing Region. *J. Geo-Inf. Sci.* **2018**, *20*, 68–78.
38. Cao, Z.; Wu, Z.; Kuang, Y.-Q.; Huang, N. Correction of DMSP/OLS night-time light images and its application in China. *J. Geo-Inf. Sci.* **2015**, *17*, 1092–1102.
39. Stedinger, J.R.; Tasker, G.D. Regional hydrologic analysis 1. ordinary, weighted, and generalized least-squares compared. *Water Resour. Res.* **1985**, *21*, 1421–1432. [[CrossRef](#)]
40. Rivera-Gonzalez, L.; Bolonio, D.; Mazadiego, L.F.; Valencia-Chapi, R. Long-Term Electricity Supply and Demand Forecast (2018–2040): A LEAP Model Application towards a Sustainable Power Generation System in Ecuador. *Sustainability* **2019**, *11*, 5316. [[CrossRef](#)]
41. Perwez, U.; Sohail, A.; Hassan, S.F.; Zia, U. The long-term forecast of Pakistan’s electricity supply and demand: An application of long range energy alternatives planning. *Energy* **2015**, *93*, 2423–2435. [[CrossRef](#)]
42. Shah, I.; Lisi, F. Day-ahead electricity demand forecasting with nonparametric functional models. In Proceedings of the 12th International Conference on the European Energy Market (EEM), Lisbon, Portugal, 19–22 May 2015.
43. Shah, I.; Iftikhar, H.; Ali, S.; Wang, D.P. Short-Term Electricity Demand Forecasting Using Components Estimation Technique. *Energies* **2019**, *12*, 2532. [[CrossRef](#)]
44. Hamdoun, H.; Sagheer, A.; Youness, H. Energy time series forecasting-analytical and empirical assessment of conventional and machine learning models. *J. Intell. Fuzzy Syst.* **2021**, *40*, 12477–12502. [[CrossRef](#)]